

Published in final edited form as:

*Nat Mater.* 2020 November 01; 19(11): 1230–1235. doi:10.1038/s41563-020-0736-2.

## Biosynthetic self-healing materials for soft machines

Abdon Pena-Francesch<sup>1</sup>, Huihun Jung<sup>2</sup>, Melik C. Demirel<sup>2</sup>, Metin Sitti<sup>1,3</sup>

<sup>1</sup>Physical Intelligence Department, Max Planck Institute for Intelligent Systems, Stuttgart, Germany

<sup>2</sup>Center for Research on Advanced Fiber Technologies (CRAFT), Materials Research Institute, Huck Institutes of the Life Sciences, and Department of Engineering Science and Mechanics, The Pennsylvania State University, University Park, PA, USA

<sup>3</sup>School of Medicine and School of Engineering, Koç University, Istanbul, Turkey

### Abstract

Self-healing materials are indispensable for soft actuators and robots that operate in dynamic and real-world environments, as these machines are vulnerable to mechanical damage. However, current self-healing materials have shortcomings that limit their practical application, such as low healing strength (below a megapascal) and long healing times (hours). Here, we introduce high-strength synthetic proteins that self-heal micro- and macro-scale mechanical damage within a second by local heating. These materials are optimized systematically to improve their hydrogen-bonded nanostructure and network morphology, with programmable healing properties (2–23MPa strength after 1s of healing) that surpass by several orders of magnitude those of other natural and synthetic soft materials. Such healing performance creates new opportunities for bioinspired materials design, and addresses current limitations in self-healing materials for soft robotics and personal protective equipment.

---

Traditional robots and actuators are typically composed of rigid and brittle materials. By contrast, in the growing field of soft robotics, flexible and largely deformable materials are explored to achieve compliance akin to that of biological systems (Young's moduli in the range of kPa to GPa)<sup>1</sup>. Compliance and complex deformation enable the soft robots to adapt to unpredictable surroundings, which makes these robots safer for physical interactions with

---

Correspondence to: Melik C. Demirel; Metin Sitti.

**Correspondence and requests for materials** should be addressed to M.C.D. or M.S. melik@psu.edu; sitti@is.mpg.de.

**Publisher's note** Springer Nature remains neutral with regard to jurisdictional claims in published maps and institutional affiliations.

**Reprints and permissions information** is available at [www.nature.com/reprints](http://www.nature.com/reprints).

#### Author contributions

A.P.-F., M.C.D., and M.S. conceived the project. A.P.-F. designed and performed the experiments, analysed the data, and wrote the manuscript. H.J. performed the protein expression and purification. All authors participated in manuscript revisions, discussions, and data interpretation.

#### Competing interests

A.P.-F. and M.C.D. have issued patents (US patent 9,663,658 and US patent 10,253,144), and H.J. and M.C.D. have issued patents (US patent 9,765,121, US patent 10,047,127, and US patent 10,246,493) on technology related to processes described in this article. All other authors have no competing interests.

#### Reporting summary

Further information on research design is available in the Nature Research Reporting Summary linked to this article.

humans and for operation in dynamic environments<sup>2,3</sup>. Although soft machines are generally resistant to blunt damage (for example, impact, compression, and bending)<sup>4</sup>, they are vulnerable to mechanical damage (puncture, tear, and cutting) owing to their inherent softness, which limits their longevity and performance<sup>5</sup>. In recent years, intense research efforts have been applied to the development of stretchable self-healing materials that recover their structure and properties after damage. Current strategies involve extrinsic self-healing through vascularization or encapsulation of healing agents<sup>6</sup>, and intrinsic self-healing either through dynamic covalent bonds as in Diels–Alder reactions<sup>7</sup> and disulfide chemistries<sup>8</sup>, or through supramolecular non-covalent chemistries such as hydrogen bonding<sup>9,10</sup>, metal ion coordination<sup>11</sup>, ionic interactions<sup>12</sup>, and van der Waals forces<sup>13</sup>. Some of these self-healing strategies have been integrated recently into soft-robotic platforms<sup>14</sup> such as soft actuators<sup>7,15</sup>, electronics<sup>16,17</sup>, and devices<sup>18</sup>. However, despite their promise, these self-healing materials still have substantial shortcomings that limit their performance and real-world applications, because they need a continuous supply of potentially hazardous monomers and catalysts, lose functionality during repair, have low mechanical strength after healing, require high energy input to trigger the self-healing, or require long healing times (often greater than 24 h).

To overcome these challenges, here we use the tools of synthetic materials biology<sup>19</sup> to rationally design synthetic tandem repeat proteins and develop strong, fast, self-healing materials for soft-robotic applications (Fig. 1a). Recently, protein engineering methodology to synthesize libraries of biomimetic sequences with controlled length by tandem repetition of amino acid building blocks and by rolling circle amplification DNA assembly was designed<sup>20</sup>. Using protein analyses across squid species<sup>20,21</sup>, biomimetic sequences inspired by proteins in squid ring teeth (predatory teeth structures inside the suction cups<sup>22,23</sup>) were designed. These proteins consist of segmented amino acid sequences with amorphous and crystal-forming blocks, which were expressed in genetically modified host organisms (bacteria) to develop protein-based functional materials with programmable properties (for example mechanical<sup>24</sup>, transport<sup>25</sup>, and thermal<sup>26</sup>). In this work, we exploit the tandem repeat design of squid-inspired synthetic proteins to generate physically crosslinked supramolecular networks (based on hydrogen bonding) with systematically controlled morphology and with self-healing properties superior to those of previously reported native proteins and other synthetic soft materials (with healing speed and strength that are several orders of magnitude higher). The self-healing performance of our biosynthetic proteins creates new opportunities, as these proteins eliminate pre-existing limitations in self-healing materials (loss of functionality, low mechanical strength after healing, and long healing times) that restricted their practical application in soft robotics previously. To illustrate these unique advantages, we demonstrate protein-based soft actuators that are capable of self-healing extreme (typically catastrophic) mechanical damage within one second, and with performance (specific work and power) superior to that of biological muscle.

## Squid-inspired biosynthetic proteins

Biosynthetic proteins with  $n = 4, 7, 11,$  and  $25$  tandem repetitions (TRs) of the squid-inspired building block (TR<sub>n</sub>4, TR<sub>n</sub>7, TR<sub>n</sub>11, and TR<sub>n</sub>25, with molecular weights of 15.8, 25.7, 39.4, and 84.6 kDa, respectively) were synthesized, spanning peptide lengths found in

native proteins and beyond (Fig. 1b). Driven by their segmented amino acid sequences, the tandem repeat polypeptides self-assemble into supramolecular  $\beta$ -sheet-stabilized networks (Fig. 1c). The nanostructure of the protein networks was identified by infrared spectroscopy and X-ray diffraction (Supplementary Figs. 1,2), which confirmed the presence of  $\beta$ -sheet structures for all the tandem repeat polypeptides. Although the tandem repeat polypeptides have the same crosslinking structures, changes in network morphology arise from the amorphous phase (which is composed of flexible chains). Protein networks can have defective morphologies caused by molecular defects such as dangling ends or loops (Supplementary Fig. 3) that degrade the material properties, which is a long-standing challenge in soft matter physics and chemistry<sup>27</sup>. A network parameter  $e_{\text{eff}} = 1 - (\beta_c/n)$ , in which  $\beta_c$  is the  $\beta$ -sheet crystallite size (average of four  $\beta$ -strands) and  $n$  is the tandem repetition of the master building block, approximates the effective strand density (the tie-chain density, or effective connections between crosslinking points) from zero (defective network) to unity (perfect network)<sup>24</sup>. Hence, by controlling tandem repetition accurately in our polypeptides ( $n = 4$  to 25), we can tailor systematically the molecular defect density from ‘all-defective’ networks (TRn4) to ‘close-to-perfect’ networks (TRn25), and optimize the network morphology beyond that of native protein complexes from squid ring teeth. Consequently, the physical properties of tandem repeat biosynthetic polypeptides, which include protein cohesion at room temperature (that is, protein-protein adhesion) (Fig. 1d), surpass those of natural and recombinant squid-derived proteins of the same family. Such control of the molecular defects enables the programming of properties by sequence design, which yields protein materials with remarkable self-healing performance (superior to that of self-healing proteins investigated in previous work<sup>28,29</sup> and other state-of-the-art synthetic self-healing materials), and provides an excellent platform to develop bio-based self-healing materials suitable for applications that require mechanical strength and fast healing kinetics.

## Self-healing mechanism and properties

Among the three major approaches of vascular, capsule-based, and intrinsic self-healing<sup>6</sup>, the mechanism of our squid-inspired polypeptides falls under intrinsic self-healing. Owing to the non-covalent nature of supramolecular interactions through hydrogen bonding, protein networks are repaired quickly after damage with physical crosslinks through chain diffusion within the protein matrix and  $\beta$ -sheet nanostructures (Fig. 2a), and the material structure, properties, and functionality are recovered. To facilitate chain diffusion and network repair, protein materials are plasticized with water (Supplementary Fig. 4). Dehydrated proteins have a glass transition temperature close to that of thermal degradation, which limits the practical use of the material in its rubbery state<sup>30</sup>. However, hydration decreases the glass transition temperature, which enables a stable rubbery state over a wide temperature range (including room temperature) (Supplementary Fig. 5). Unlike in other chemistries that require melting and re-forming of physical crosslinking structures, melting during the protein healing process is not observed in bulk ( $\beta$ -sheets melt at high temperatures beyond thermal degradation in similar structural proteins)<sup>31</sup>. This was confirmed by mechanical analysis (see Supplementary Fig. 6) and structural analysis (see Supplementary Figs. 1,2), which revealed that the physically crosslinked network was not disrupted during healing. For our protein-based materials, this process has a major advantage over other chemistries

because mechanical stability is not lost during the healing process and the global network structure does not need to re-form from a molten or liquid state, which enables faster healing.

To understand the strength and kinetics of the healing process in our bioinspired protein system, we investigated the cohesion between two hydrated protein surfaces (Supplementary Fig. 7). We analysed systematically the cohesion as a function of contact time (Supplementary Fig. 8), hydration (Supplementary Fig. 9), preload (Supplementary Fig. 10), temperature, and network morphology (Supplementary Fig. 11). Polypeptides showed good cohesion with increasing network parameter  $\epsilon_{\text{eff}}$  owing to network and chain connectivity optimization (Supplementary Figs. 11,12). Moreover, polypeptides exhibited strong but slow healing at room temperature (23 °C), and soft but fast healing at temperatures above 45 °C (Supplementary Fig. 13). As temperature increases, so does the protein chain mobility<sup>26</sup>, which softens the material and facilitates the fast diffusion of chain segments across the separated parts. Therefore, although healing occurs already at room temperature, temperature regulation offers control over the healing kinetics for a tailored performance. For example, for optimized kinetics and strength, the healing can be accelerated by raising the temperature to 50 °C and then strengthened by cooling back to room temperature. Such temperature-accelerated healing behaviour can be exploited to develop fast, high-strength, self-healing strategies for protein-based materials (Supplementary Video 1). This represents a major advantage over other self-healing chemistries, which typically require long healing times to repair the damaged material (often greater than 24 h). Long healing times hinder the use of self-healing materials in many applications because the material loses its functionality during the repair process (that is, the material is weak while it heals) and exhibits low mechanical strength (healing times typically greater than 1 h are required for mechanical strength of at least 1 MPa). Our polypeptide materials exhibit mechanical strength up to  $23 \pm 1$  MPa after extremely short healing times ( $\sim 1$  s) (Supplementary Fig. 14). Such reduced healing time and superior healing strength position our biosynthetic squid-inspired proteins in a previously unexplored area of performance in self-healing soft materials (Fig. 2b and Supplementary Data 1), and provide a solution for previous limitations in healing time and strength.

## Healing of extreme mechanical damage

Validation of self-healing varies greatly depending on the type of material, the nature of the damage, the material properties, and the intended application (such as scratches in thin films and coatings<sup>32</sup>, punctures in soft electronics<sup>16</sup>, cuts in elastomers<sup>10</sup>, and cracks in composites<sup>33</sup>)<sup>6</sup>. With the intention of providing a broad testbed for our materials, we validated the self-healing properties of tandem repeat polypeptides against different types of severe mechanical damage that are fatal in soft material and actuator performance. Damaged protein materials were healed either by locally heating the damaged area through mechanical contact (Supplementary Figs. 15,16) or by bulk-heating the entire material in a temperature-controlled chamber (Supplementary Fig. 17), both at 50 °C and for a short duration of time.

Scratch damage of coated surfaces typically results in the deterioration of the protective coating layer, which exposes the underlying substrate to environmental contamination (and

leads to corrosion, biofouling, and overall failure of sensing interfaces). Protein-coated substrates (Fig. 3a) were laser-micromachined to simulate a scratch defect pattern, and were locally (half defect) and fully (complete defect) healed for 2 s consecutively. After the short healing process, the damaged protein recovered its conformal surface coverage and the underlying substrate was protected again by the healed coating (better post-healing homogeneity could be achieved with longer healing processes).

Puncture damage (hole or point defect) are problematic in pressurized systems that are typically used in microfluidics and soft robotics, because a small defect can cause the leakage of internal fluid or air and cancel the functions of the device. We punctured a free-standing, flexible TRn11 protein film (50  $\mu\text{m}$  thick) to create a hole defect, which was healed in less than 1 s by local heating of the damaged area (Fig. 3b). We note that intrinsic self-healing mechanisms are limited to small damage volumes because there is no transport of new material to the damaged area (unlike in vascular or encapsulation self-healing mechanisms, in which healing agents are typically fed to the damaged areas)<sup>6</sup>. This limitation becomes important when a high volume of material is removed, as in hole-punch defects. In this case, the healing is limited by the defect size and viscoelasticity of the material (Supplementary Fig. 18). However, such a size limitation can be bypassed by patching, which enables the healing of large-scale defects by the incorporation of new protein material.

Finally, we evaluated the healing of total cut damage, in which the damaged protein material was separated completely into two pieces and the healing was then assessed (Fig. 3c). Free-standing films of cut-damaged protein were healed within 1 s, recovered their elastomeric properties, and exhibited stretching deformations greater than 200% strain and post-healing strength of up to 23 MPa for high-repetition tandem repeat polypeptides (Supplementary Fig. 14)<sup>24</sup>. Healing of thick bulk protein samples was also demonstrated directly through cut surfaces (Supplementary Fig. 19). After being stretched until failure, the samples did not break at the healed area but broke at random non-healed regions, which indicates that the healing of total cut defects was effective and that the healed regions were at least as strong as the pristine material.

In summary, the tandem repeat polypeptides showed outstanding self-healing performance for a variety of extreme damage types after very brief healing times, which makes them an excellent material for soft-robotic applications that require adaptation to dynamic environments and self-repair.

## Self-healing protein actuators for soft robotics

To explore the use of self-healing bioinspired tandem repeat proteins in soft actuators and robotics, we designed and built a pneumatic soft actuator that consists of two protein disc membranes joined together at the perimeter and connected to a pneumatic circuit (Fig. 4a). When the actuator is pressurized, the soft TRn11 protein membranes deform and the actuator expands in volume, which causes a deformation and a force output that is normal to the membrane (Fig. 4b, Supplementary Video 2). Although our protein material can be used in other soft actuator designs and other actuation mechanisms<sup>34</sup>, we demonstrate pneumatic

actuation because it is a well-established and common actuation mechanism in soft robotics, and because pneumatic actuators are especially vulnerable to puncture damage<sup>35</sup>. We analysed the performance (displacement and force output) of a single-chamber protein actuator before damage (pristine) and after puncture damage and healing (healed) (Fig. 4c). With a maximum displacement of 10 mm (400% actuation strain) and a force output of 5 N for a single-chamber actuator in its current design, the same performance was observed in pristine and healed actuators. The healing of the protein membranes can repair the defects effectively, and therefore extend the operational lifetime of the actuators beyond unpredictable damage.

Although the performance of our pneumatic actuator could be improved further by optimizing the design and fabrication for specific tasks, actuation types, and specific output metrics<sup>1,34</sup>, the current non-optimized soft actuator design can be used in its present form in diverse soft-robotic applications. In a proof-of-concept demonstration, we used two opposing soft protein actuators to build a soft gripper (Fig. 4d and Supplementary Video 3), which is a promising application of soft robotics in food, pharmaceutical, packaging, and retail industries<sup>35,36</sup>. Owing to the compliance of the protein membranes, the gripper can adapt to complex geometries and exert friction force to manipulate delicate objects (a cherry tomato, in this pick-and-place example)<sup>37</sup>. Next, using the same protein soft actuator design, we built an artificial muscle capable of lifting repeatedly a dead weight at least 3,000 times heavier than its own mass (Fig. 4e, Supplementary Video 4 and Supplementary Note 1). In its current design, the protein muscle has a specific work of 215 J kg<sup>-1</sup>, an average specific power of 488 W kg<sup>-1</sup>, and a thermodynamic efficiency of 62% (Supplementary Note 1 and Supplementary Fig. 20), which exceed those of biological muscle and are comparable to those of other state-of-the-art soft actuators (Supplementary Data 2)<sup>34,38–40</sup>.

In addition to their versatility, high performance, and self-healing capabilities, tandem repeat polypeptide actuators are also chemically recyclable. On-demand degradation of protein-based robots and actuators is essential for sustainability (no pollution or electronic waste at the end of their functional lifetime) and healthcare applications (biodegradation in the body to avoid retrieval procedures)<sup>41</sup>. The protein material can degrade due to enzymatic activity (proteolysis) or due to the disruption of its nanostructure, spanning a wide range of degradation kinetics. Taking advantage of the protein non-covalently crosslinked (hydrogen-bonded) network, we have demonstrated the fast dissolution of the protein actuator (Fig. 4f and Supplementary Video 5). Although the protein membranes of the soft actuator are stable and operate normally underwater, they start to dissolve after a pH stimulus (acetic acid to a concentration of 5% v/v) is administered, which breaks the  $\beta$ -sheet nanostructures<sup>42</sup>. The membrane is initially degraded in less than half a minute (loss of functionality), and the actuator is fully dissolved in less than five minutes. The degradation process can be tailored for slower or faster kinetics and activated by different stimuli and biomolecules<sup>42</sup>, which offers a wide range of degradation profiles for different applications (that is, slow degradation that conserves the functionality of the robot or actuator for long time periods versus flash destruction of the device).

The healing performance of tandem repeat polypeptides creates new opportunities for the design of bioinspired and biosynthetic materials that were not possible previously, and

addresses current limitations in self-healing soft materials (that is, low mechanical strength and long healing times, often longer than 24 h, versus high mechanical strength after healing in a few seconds). We fabricated protein-based, versatile, biodegradable, and self-healing soft actuators with performance comparable to that of state-of-the-art soft actuators and exceeding that of biological muscle, and we have demonstrated their use in soft gripping and artificial muscle technologies. These protein-based materials can heal severe mechanical damage (for example, scratch, puncture, and total cut damage), and can be integrated easily in other actuator designs and potentially in other soft systems and machines with different actuation and healing methods, which will be the focus of our future work. Biosynthetic protein materials present a promising platform for bringing soft robotics closer to simulating complex biological systems, and open a wide design space for multifunctional soft machines with properties traditionally associated exclusively with living systems, such as adaptation to external hazards, fast self-healing, and degradation at the end of the functional lifetime.

## Online content

Any methods, additional references, Nature Research reporting summaries, source data, extended data, supplementary information; acknowledgements, peer review information, details of author contributions and competing interests; and statements of data and code availability are available at <https://doi.org/10.1038/s41563-020-0736-2>.

## Methods

### Biosynthesis of squid-inspired proteins

Biosynthetic proteins were constructed and expressed based on protocols described in previous work<sup>20</sup>. In brief, a DNA sequence encoding a YGYGGLYGGLYGGLGYPAAASVSTVHHP amino acid building block was constructed based on consensus derived from analysis of multiple squid species. DNA constructs with a precise number  $n$  of building block repeats were generated by protected digestion rolling circle amplification. Selected constructs of tandem repeat polypeptides (TRn4, TRn7, TRn11, and TRn25) were ligated to an expression vector to create an expression library for squid-inspired protein biosynthesis in *Escherichia coli* bacteria. Native proteins were extracted from *Loligo vulgaris* squid from Tarragona, Spain<sup>43</sup>. Protein size was confirmed by polyacrylamide gel electrophoresis.

### Fabrication of protein-based materials

Biosynthetic tandem repeat polypeptides and native proteins were dissolved overnight in 1,1,1,3,3,3,-hexafluoro-2-propanol to a concentration of 50 mg ml<sup>-1</sup>. The protein solution was cast into polydimethylsiloxane moulds and on silica glass substrates to fabricate free-standing protein films and protein-coated substrates for characterization and healing analysis. In addition, protein films were cut to specified computer-aided design geometries for characterization and device fabrication in a laser micromachining system (LPKF ProtoLaser U3). Some protein films were doped with dyes (brilliant green, disperse red, or fluorescein, < 1% w/w) for enhanced visualization and contrast.

### Protein structure analysis

Fourier transform infrared spectroscopy of pristine and healed protein samples was performed in a Bruker Tensor II spectrometer with a Platinum ATR accessory (256 scans with  $4\text{ cm}^{-1}$  resolution). X-ray diffraction analysis was performed in a Rigaku D/MAX RAPID II microdiffractometer ( $\lambda = 0.154\text{ nm}$ ) with a Cu K $\alpha$  source and a  $30\text{ }\mu\text{m}$  collimator at 50 kV and 40 mA. Absorption band and diffraction peak analyses were performed as described previously<sup>20</sup>.

### Water absorption in proteins

The water content of hydrated proteins was measured by thermogravimetric analysis (TGA) and simultaneous mass spectrometry that were performed on a TA Instruments Q50 TGA instrument coupled to a Pfeiffer vacuum mass spectrometer. Protein samples were hydrated by immersion in deionized water for 10 min at room temperature, and then excess water was removed by blotting. Samples were heated from room temperature to  $500\text{ }^{\circ}\text{C}$  at a heating rate of  $10\text{ }^{\circ}\text{C min}^{-1}$  in a helium environment ( $90.0\text{ ml min}^{-1}$  flow). Representative  $m/z$  17,  $m/z$  18, and  $m/z$  44 ion signals were monitored to identify water evaporation and protein thermal degradation.

### Thermal characterization

Temperature-modulated differential scanning calorimetry was performed on a TA Instruments DSC 2500 calorimeter with hermetic Tzero pans. Dehydrated samples were obtained by drying for 1 h at  $80\text{ }^{\circ}\text{C}$ , whereas hydrated samples were obtained by immersion in deionized water for 10 min and blotting to remove excess water. Dehydrated and hydrated samples were measured from  $-90\text{ }^{\circ}\text{C}$  to  $190\text{ }^{\circ}\text{C}$  and from  $-90\text{ }^{\circ}\text{C}$  to  $70\text{ }^{\circ}\text{C}$ , respectively. Samples were heated at a rate of  $2\text{ }^{\circ}\text{C min}^{-1}$  with a modulation amplitude of  $0.32\text{ }^{\circ}\text{C}$  and period of 60 s.

### Mechanical characterization

Pristine and healed protein dog-bone-shaped specimens ( $15\text{ mm}$  gauge length  $\times$   $4\text{ mm}$  width  $\times$   $50\text{ }\mu\text{m}$  thickness) were characterized in an Instron 5866 load frame with a 10 N cell (accuracy  $\pm 0.3\%$ ) and a custom-built immersion chamber. Samples were stretched at a rate of  $5\text{ mm min}^{-1}$ . Dynamic properties were measured in a TA Instruments Discovery HR-2 rheometer with a dynamic mechanical analysis accessory (film tension mode) and with a parallel plate geometry in a temperature-controlled water bath.

### Protein cohesion and healing kinetics

Healing kinetics experiments were performed in the TA Instruments Discovery HR-2 rheometer with a customized setup (Supplementary Fig. 7). Glass substrates with  $10\text{ mm}$  outer diameter were adhered to disposable rheometer plates and were coated with  $20\text{ mg}$  of protein. The measurements were performed in a liquid cell, which enabled testing under hydrated and dehydrated conditions, over a temperature range of  $10\text{--}80\text{ }^{\circ}\text{C}$ , with different preloads ( $1\text{--}242\text{ kPa}$ ), and with different contact times ( $1\text{--}625\text{ s}$ ). The protein-coated surfaces were loaded at a speed of  $5\text{ }\mu\text{m s}^{-1}$  to a variable loading force, held during a variable contact time ( $1, 5, 11, 25, 56, 125, 280,$  and  $625\text{ s}$ ), and unloaded at a speed of  $20$



$\mu\text{m s}^{-1}$ . The maximum unloading adhesion force was measured as function of contact time and temperature, and was used in the calculations of healing prefactor  $c_{\text{healing}}$ .

### Protein healing

In experiments with local healing, samples were hydrated and heated locally to 50 °C with a hot tip from an 80 W Weller PU 81 soldering station with adjustable temperature (Supplementary Fig. 14). A polydimethylsiloxane spacer (400  $\mu\text{m}$  thick) was used to prevent sample adhesion or contamination, and temperature was controlled with a type K thermocouple. The damaged areas were pressed gently with the hot tip for a short duration (typically 1 s, depending on damage volume). In experiments with bulk healing, hydrated samples were placed in a heating chamber at 50 °C.

### Types of mechanical damage of protein materials

Protein films of 50  $\mu\text{m}$  thickness (either free-standing or integrated in the soft actuator) were pierced with a 24 gauge needle to simulate puncture damage. Punch-hole defects were created with a 5 mm outer diameter Rapid-Core sampling tool. To simulate scratch damage, protein-coated glass substrates (100  $\mu\text{m}$  coating thickness) were laser-cut with a predesigned pattern in the LPKF laser micromachining system at 0.189 W and 50 kHz. To simulate total cut damage, protein films, dog-bone-shaped specimens for mechanical analysis, and bulk protein samples were cut with a razor blade into two separate half pieces. In all cases, after damage, healing was performed with local or bulk healing as described previously.

### Surface roughness

Protein films (pristine and healed) were dried at room temperature and their surface roughness was measured by 3D laser scanning microscopy (Keyence VK-X200).

### Protein soft actuator

Two protein discs (30 mm outer diameter, 50  $\mu\text{m}$  thick) were mounted in a ring holder and connected to a pneumatic circuit. The pneumatic actuator was controlled by a 60 ml syringe and a Panasonic DP-100 pressure sensor. The actuator deformation was recorded with a Sony HDR-CX900 camera at 25 fps, and force output was measured in a TA Instruments Discovery HR-2 rheometer. The actuator was puncture-damaged with a needle and healed locally as described above. The soft gripper was fabricated by mounting two opposed protein actuators on an adjustable frame. The artificial muscle was fabricated by mounting a hook on the outer protein membrane. For actuator degradation, the protein films were doped with 1% (w/w) fluorescein for visualization under ultraviolet light. The protein actuator was mounted in a liquid cell with water, and acetic acid (for pH stimulus) was administered to a total concentration of 5% (v/v).

### Supplementary Material

Refer to Web version on PubMed Central for supplementary material.

## Acknowledgements

The authors thank H. Shahsavan and P. Cabanach for helpful discussions. M.C.D. and H.J. thank staff members of Penn State MRI and Huck user facilities. A.P.-F. and M.S. were supported by the Max Planck Society. A.P.-F. was also funded by the Alexander von Humboldt Foundation and the German Federal Ministry for Education and Research. M.S. was also funded by the European Research Council (ERC) Advanced Grant SoMMoR project with grant no: 834531. M.C.D. and H.J. were supported by the United States Army Research Office (grant no. W911NF-16-1-0019 and W911NF-18-1-026) and the Huck Endowment of The Pennsylvania State University.

## Data availability

All relevant data that support the findings of this study are available in the article and its supplementary files. Source data for Figs. 1b,1c,4c are available in the Source Data files. Additional data can be obtained from the authors upon request.

## References

1. Rus D, Tolley MT. Design, fabrication and control of soft robots. *Nature*. 2015; 521:467–475. [PubMed: 26017446]
2. Hu W, Lum GZ, Mastrangeli M, Sitti M. Small-scale soft-bodied robot with multimodal locomotion. *Nature*. 2018; 554:81–85. [PubMed: 29364873]
3. Ren Z, Hu W, Dong X, Sitti M. Multi-functional soft-bodied jellyfish-like swimming. *Nat Commun*. 2019; 10:2703. [PubMed: 31266939]
4. Martinez RV, Glavan AC, Keplinger C, Oyetibo AI, Whitesides GM. Soft actuators and robots that are resistant to mechanical damage. *Adv Funct Mater*. 2014; 24:3003–3010.
5. Yang G-Z, et al. The grand challenges of Science Robotics. *Sci Robot*. 2018; 3
6. Blaiszik BJ, et al. Self-healing polymers and composites. *Annu Rev Mater Res*. 2010; 40:179–211.
7. Terryn S, Brancart J, Lefeber D, van Assche G, Vanderborcht B. Self-healing soft pneumatic robots. *Sci Robot*. 2017; 2
8. Canadell J, Goossens H, Klumperman B. Self-healing materials based on disulfide links. *Macromolecules*. 2011; 44:2536–2541.
9. Cordier P, Tournilhac F, Soulié-Ziakovic C, Leibler L. Self-healing and thermoreversible rubber from supramolecular assembly. *Nature*. 2008; 451:977–980. [PubMed: 18288191]
10. Chen Y, Kushner AM, Williams GA, Guan Z. Multiphase design of autonomic self-healing thermoplastic elastomers. *Nat Chem*. 2012; 4:467–472. [PubMed: 22614381]
11. Li C-H, et al. A highly stretchable autonomous self-healing elastomer. *Nat Chem*. 2016; 8:618–624. [PubMed: 27219708]
12. Cao Y, et al. A transparent, self-healing, highly stretchable ionic conductor. *Adv Mater*. 2017; 29
13. Urban MW, et al. Key-and-lock commodity self-healing copolymers. *Science*. 2018; 362:220–225. [PubMed: 30309952]
14. Bilodeau RA, Kramer RK. Self-healing and damage resilience for soft robotics: a review. *Front Robot AI*. 2017; 4:48.
15. Acome E, et al. Hydraulically amplified self-healing electrostatic actuators with muscle-like performance. *Science*. 2018; 359:61–65. [PubMed: 29302008]
16. Markvicka EJ, Bartlett MD, Huang X, Majidi C. An autonomously electrically self-healing liquid metal-elastomer composite for robust soft-matter robotics and electronics. *Nat Mater*. 2018; 17:618–624. [PubMed: 29784995]
17. Tan YJ, et al. A transparent, self-healing and high- $\kappa$  dielectric for low-field-emission stretchable optoelectronics. *Nat Mater*. 2020; 19:182–188. [PubMed: 31844282]
18. Huynh T-P, Sonar P, Haick H. Advanced materials for use in soft self-healing devices. *Adv Mater*. 2017; 29
19. Roberts AD, et al. Synthetic biology for fibers, adhesives, and active camouflage materials in protection and aerospace. *MRS Commun*. 2019; 9:486–504. [PubMed: 31281737]

20. Jung H, et al. Molecular tandem repeat strategy for elucidating mechanical properties of high-strength proteins. *Proc Natl Acad Sci*. 2016; 113:6478–6483. [PubMed: 27222581]
21. Guerette PA, et al. Accelerating the design of biomimetic materials by integrating RNA-seq with proteomics and materials science. *Nat Biotechnol*. 2013; 31:908–915. [PubMed: 24013196]
22. Nixon M, Dilly PN. Sucker surfaces and prey capture. *Symp Zool Soc Lond*. 1977; 38:447–511.
23. Pena-Francesch A, Demirel MC. Squid-inspired tandem repeat proteins: functional fibers and films. *Front Chem*. 2019; 7:69. [PubMed: 30847338]
24. Pena-Francesch A, et al. Mechanical properties of tandem-repeat proteins are governed by network defects. *ACS Biomater Sci Eng*. 2018; 4:884–891. [PubMed: 33418772]
25. Pena-Francesch A, et al. Programmable proton conduction in stretchable and self-healing proteins. *Chem Mater*. 2018; 30:898–905.
26. Tomko JA, et al. Tunable thermal transport and reversible thermal conductivity switching in topologically networked bio-inspired materials. *Nat Nanotechnol*. 2018; 13:959–964. [PubMed: 30104620]
27. Zhong M, Wang R, Kawamoto K, Olsen BD, Johnson JA. Quantifying the impact of molecular defects on polymer network elasticity. *Science*. 2016; 353:1264–1268. [PubMed: 27634530]
28. Sariola V, et al. Segmented molecular design of self-healing proteinaceous materials. *Sci Rep*. 2015; 5
29. Ding D, et al. From soft self-healing gels to stiff films in suckerin-based materials through modulation of crosslink density and  $\beta$ -sheet content. *Adv Mater*. 2015; 27:3953–3961. [PubMed: 26011516]
30. Bier JM, Verbeek CJR, Lay MC. Thermal transitions and structural relaxations in protein-based thermoplastics. *Macromol Mater Eng*. 2014; 299:524–539.
31. Cebe P, et al. Beating the heat - fast scanning melts silk beta sheet crystals. *Sci Rep*. 2013; 3:1130. [PubMed: 23350037]
32. Cho SH, White SR, Braun PV. Self-healing polymer coatings. *Adv Mater*. 2009; 21:645–649.
33. White SR, et al. Autonomic healing of polymer composites. *Nature*. 2001; 409:794–797. [PubMed: 11236987]
34. Hines L, Petersen K, Lum GZ, Sitti M. Soft actuators for small-scale robotics. *Adv Mater*. 2017; 29
35. Ilievski F, Mazzeo AD, Shepherd RF, Chen X, Whitesides GM. Soft robotics for chemists. *Angew Chem Int Ed*. 2011; 50:1890–1895.
36. Song S, Drotlef D-M, Majidi C, Sitti M. Controllable load sharing for soft adhesive interfaces on three-dimensional surfaces. *Proc Natl Acad Sci*. 2017; 114:E4344–E4353. [PubMed: 28507143]
37. Josie H, et al. Soft manipulators and grippers: a review. *Front Robot AI*. 2016; 3:69.
38. Madden JDW, et al. Artificial muscle technology: physical principles and naval prospects. *IEEE J Ocean Eng*. 2004; 29:706–728.
39. Miriyev A, Stack K, Lipson H. Soft material for soft actuators. *Nat Commun*. 2017; 8:596. [PubMed: 28928384]
40. Rich SI, Wood RJ, Majidi C. Untethered soft robotics. *Nat Electron*. 2018; 1:102–112.
41. Baumgartner M, et al. Resilient yet entirely degradable gelatin-based biogels for soft robots and electronics. *Nat Mater*. 2020; doi: 10.1038/s41563-020-0699-3
42. Pena-Francesch A, Giltinan J, Sitti M. Multifunctional and biodegradable self-propelled protein motors. *Nat Commun*. 2019; 10
43. Pena-Francesch A, et al. Materials fabrication from native and recombinant thermoplastic squid proteins. *Adv Funct Mater*. 2014; 24:7401–7409.

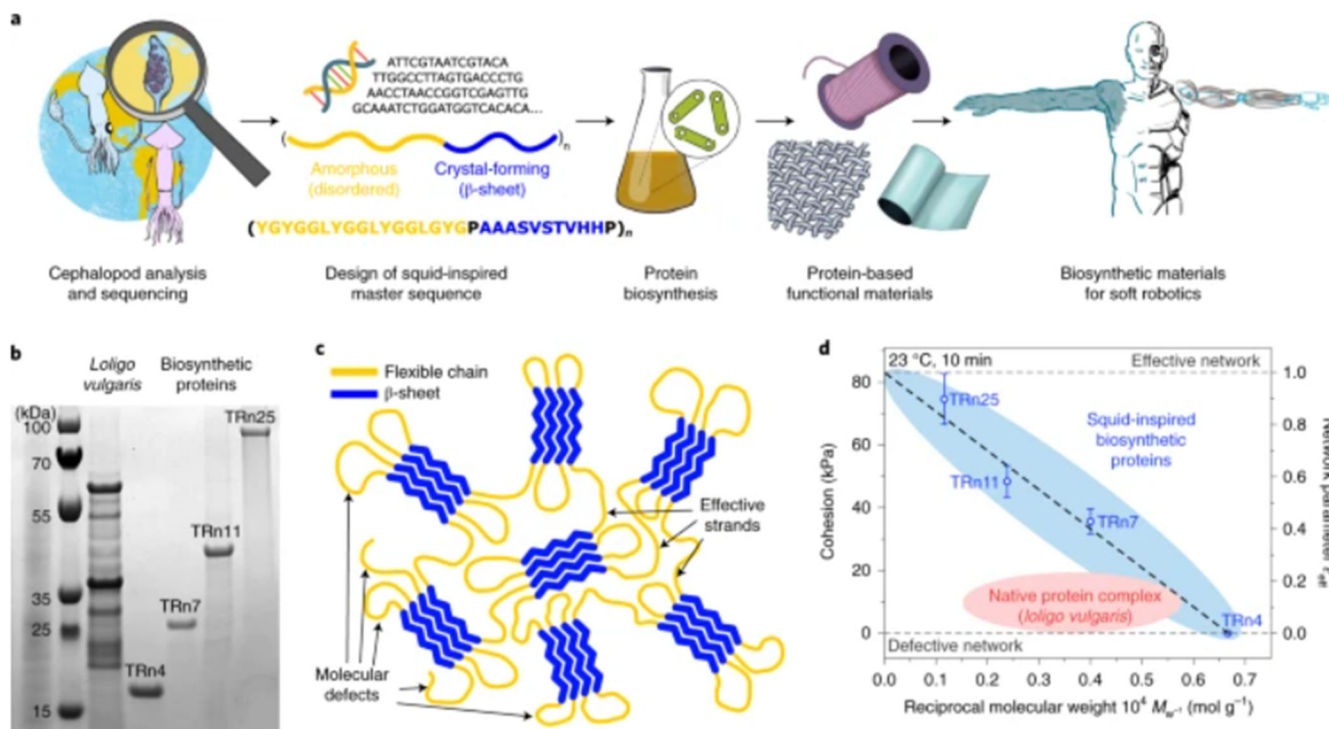


**Fig. 1. Cephalopod-inspired biosynthetic proteins.**

**a**, The analysis of squid proteins, design of a squid-inspired master sequence, and biosynthesis of protein libraries yield protein-based functional self-healing materials for soft actuators and robotics applications. **b**, Protein sizes of native *Loligo vulgaris* protein complex and biosynthetic TRn4, TRn7, TRn11, and TRn25 polypeptides. (Source Data Fig. 1b). **c**, The nanostructure of biosynthetic tandem repeat polypeptides is composed of a  $\beta$ -sheet nanocrystal network (blue) connected by flexible chains (yellow), with molecular defects (dangling ends and loops). **d**, Self-healing properties of squid-inspired proteins (at room temperature) improved beyond those of native proteins owing to an optimized network morphology. Error bars, standard deviation ( $n = 5$ ).

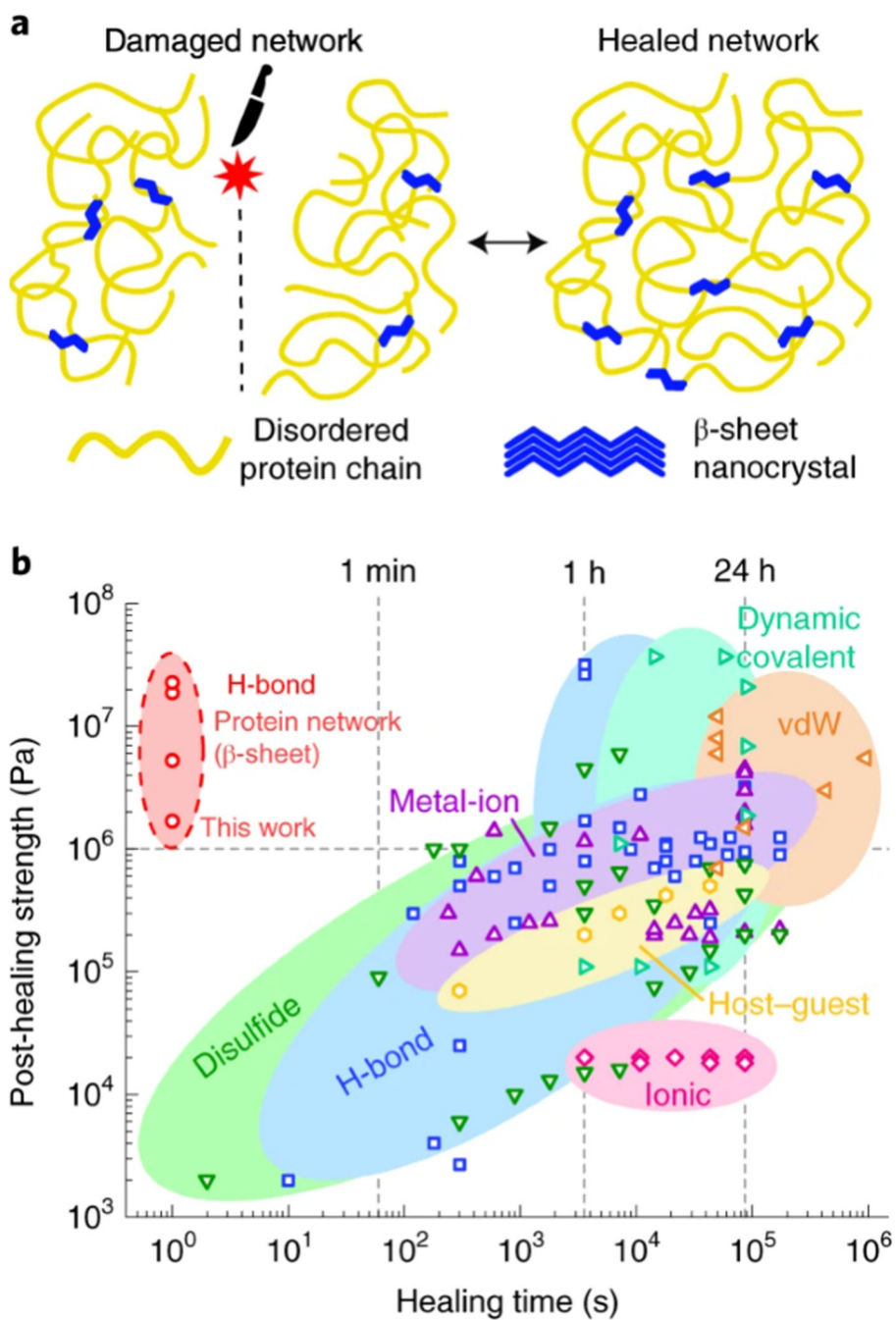


**Fig. 2. Self-healing polypeptides.**

**a.** The self-healing mechanism relies on  $\beta$ -sheet nanocrystals, which act as physical crosslinks, and diffusion across the damaged areas. **b.** The performance of squid-inspired self-healing proteins is compared to that of state-of-the-art self-healing materials (see Supplementary Data 1 for references) that use different chemistries. This provides a benchmark for self-healing materials.

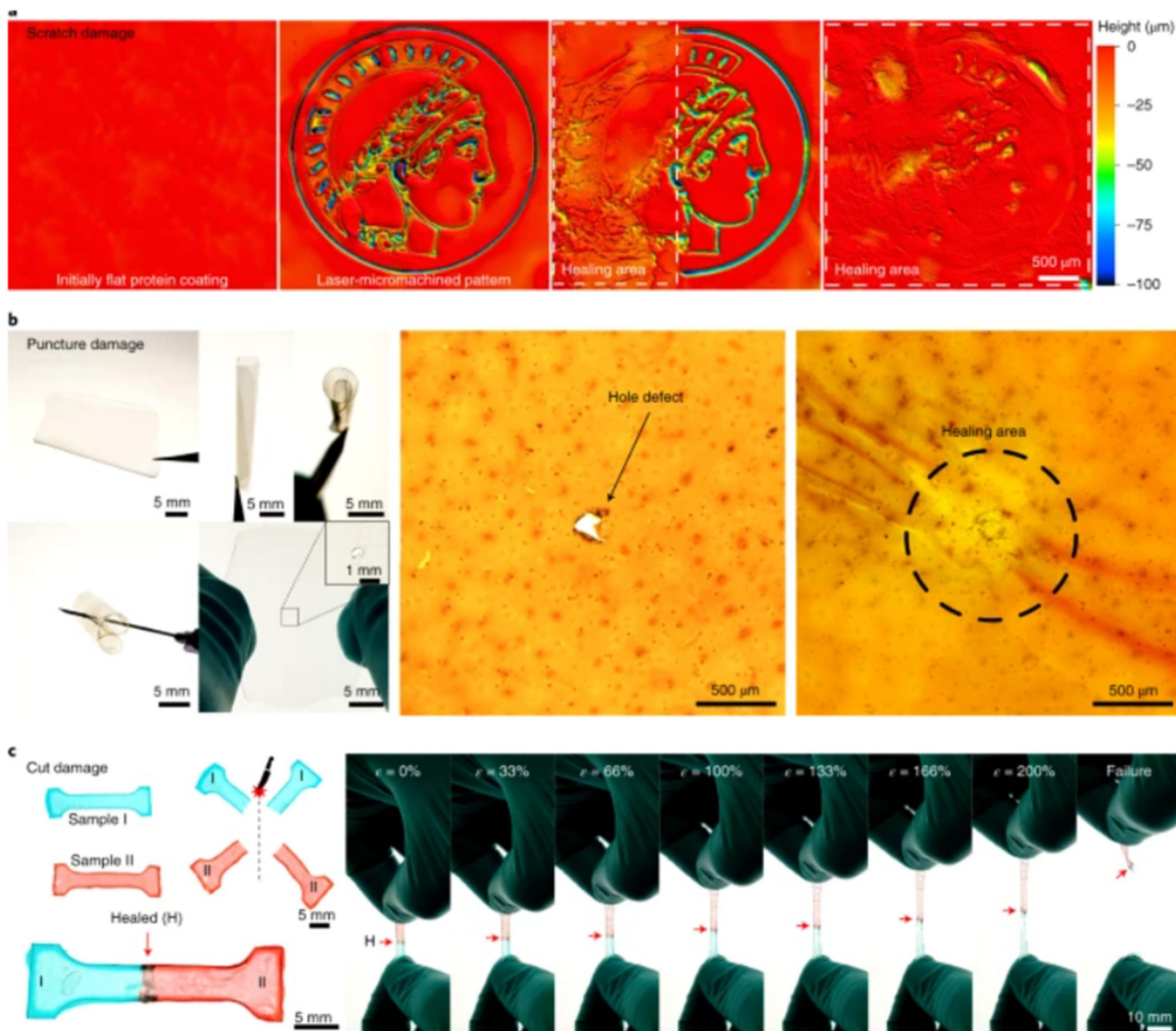


**Fig. 3. Self-healing of extreme mechanical damage.**

**a,** Scratch damage on TRn11 protein-coated substrates was partially and totally healed, each healing requiring less than 2 s. **b,** Puncture damage of free-standing, flexible TRn11 protein films (by a needle through the film) was healed in less than 1 s. **c,** Total cut damage of TRn11 protein dog-bone-shaped samples (I and II) was healed in less than 1 s. Healed samples withstand large deformations of up to 200% stretching strain before failure from a random pristine location, and healed areas are at least as strong as pristine areas.

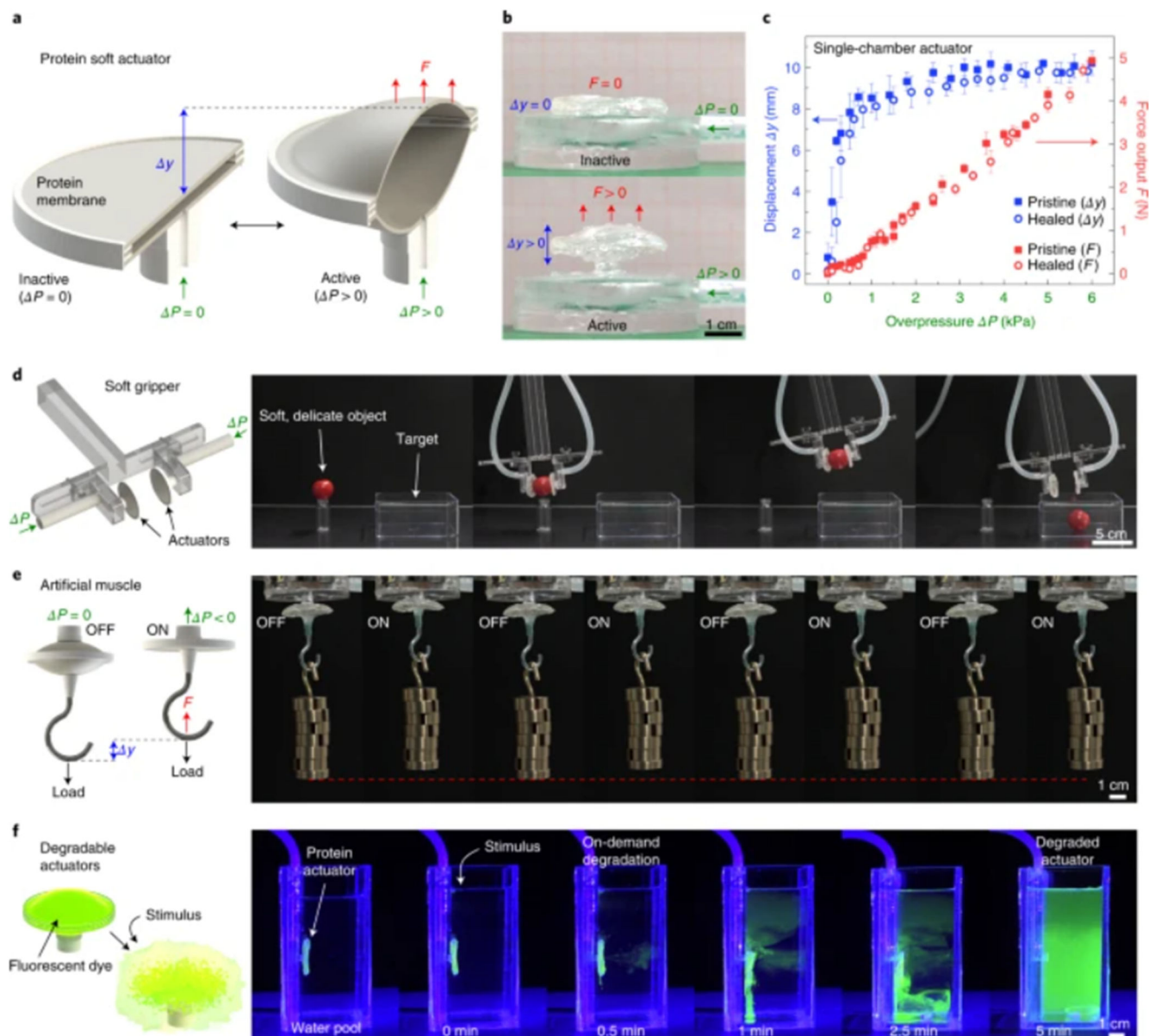


**Fig. 4. Self-healing, protein-based soft actuator.**

**a,b**, Schematic and images of a soft pneumatic actuator fabricated from TRn11 protein disc membranes. **c**, A single-chamber actuator achieves 400% strains and 5 N force output, with no distinguishable difference in performance between pristine and puncture-healed actuators. Error bars, standard deviation ( $n = 5$ ). (Source Data Fig. 4c) **d**, Soft gripper fabricated from two opposed protein actuators, capable of gripping soft, delicate objects (for example, a cherry tomato). **e**, Protein-based artificial muscle, with performance exceeding that of biological muscle. **f**, On-demand degradation of protein actuators by induced pH stimulus, which causes them to vanish at the end of their functional life (photodye added for enhanced visualization).